Cover Page

- DOE Final Report
- Grant number: DE-SC0010594
- Name of the recipient (Northwestern University)
- Project period (08/15/2013 – 08/14/2018)

- Project title: **MICROSTRUCTURE ANISOTROPY EFFECTS ON FRACTURE AND FATIGUE MECHANISMS IN SHAPE MEMORY ALLOY MARTENSITES**

- PI name: L. Catherine Brinson
  Co-PI: Aaron Stebner

DOE Final report
DE-SC0010594; PI- Catherine L. Brinson SP0022534
Report number: DOE-NU-0010594 (self-assigned)

Abstract:
The chief scientific object was to investigate the fatigue and fracture mechanisms in NiTi shape memory alloys, in the presence of stress concentrating factors such as micro-pores and notches. In particular, the interactions between structure (factors related to the geometry of the specimen, such as holes, pores and notches) and microstructure (related to properties of the material such as grains, secondary phases, twins) in influencing the inelastic deformation, leading up to fracture in NiTi was examined. Primarily, there were two major thrusts. The first thrust focused on fracture behavior in Shape Memory Alloys where the high crystal symmetry cubic phase transformed into the low symmetry phase during deformation and propagation of cracks. This thrust revealed the interplay between size of micro-pores, size of grains and grain orientations in determining the resistance to crack growth, during cyclic tensile deformation of porous-like NiTi specimens. The role of secondary phases (impurities of Ti, often formed during fabrication) were also shown to induce local inelastic deformation gradients during tensile deformation and reduce overall extent of deformation.

The second thrust focused on the fatigue and fracture behavior in the low crystal symmetry martensite phase. Unlike high symmetry phases, characterization of deformation in low symmetry phases such as martensitic NiTi has been challenging, due to a hierarchical microstructure spanning from nanoscale twins to the macroscale, a highly anisotropic microstructure stemming from the low crystal symmetry and a multitude of inelastic mechanisms for deformation. Thus, advanced X-ray techniques such as 3D high-energy diffraction microscopy and x-ray micro-Laue diffraction and spectroscopy were used in conjunction with traditional techniques such as SEM and TEM to understand the inelastic deformation in the martensite phase in NiTi, in the presence of notches. This thrust revealed a stark difference in deformation mechanisms based on the nature of stress: regions near the notch experience a highly triaxial stress while those far away experience a uniaxial stress. Additionally, while regions close to the notch were shown to deform locally by amorphization/nanocrystallization, ultimately leading to fracture, regions far away from the notch deformed in a more traditional manner, with detwinning and twin reorientation the primary mechanisms of deformation. More importantly, this thrust revealed that in the presence of structural factors such as notches, the traditional picture of reorientation (coalescence) of nanoscale martensite twins into increasingly larger domains with increased loading does not hold true, even up to fracture of the specimen.

These conclusions will inform the modeling and understanding of deformation behavior of specimens, where structure and microstructure coexist and interact.

Keywords:
shape memory alloys, size effects, martensite, structure-microstructure, notch deformation

List of citations for related documents:

- Paul, P.P. Paranjape, H.M. Nobumichi, T. Chumlyakov, Y.I. Brinson, L.C. "In-situ, microscale characterization of heterogeneous deformation around notch in martensitic Shape Memory Alloy" 2019, Materials Science and Engineering: A (in press).
- Paranjape, H.M., Paul, P.P., Amin-Ahmadi, B., Sharma, H., Dale, D., Ko, J.Y.P., Chumlyakov, Y.I., Brinson, L.C., Stebner, A.P. "In Situ 3D Characterization of the Deformation Mechanics of a Superelastic NiTi Shape Memory Alloy Single Crystal under Multiscale Constraint," 2018, *Acta Materialia*, 144:748–757, 10.1016/j.actamat.2017.11.026.
- Paul, P.P., Fortman, M., Paranjape, H.M., Anderson, P.M., Stebner, A.P., Brinson, C.L. "Influence of Structure and Microstructure on Deformation Localization and Crack Growth in NiTi Shape Memory Alloys," 2018, *Shape Memory and Superelasticity*, 4(2):285–293, 10.1007/s40830-018-0172-1.
- Paul, P.P. Paranjape, H.M., Amin-Ahmadi, B., Pagan D.C., Chumlyakov, Y.I. Brinson, L.C. "Heterogeneity and Inelasticity of Multiscale Deformation in a Notched Martensitic NiTi Shape Memory Alloy Specimen" 2019, Acta Materialia (In review).
- Paul, P.P., Kabirifar, P, Sun, Q.P., Brinson, L.C. "Structure-microstructure interactions in compression deformation of NiTi shape memory alloy micropillars," 2019, Materials Letters, 257:126693, https://doi.org/10.1016/j.matlet.2019.126693.
- Amin-Ahmadi, B., Noebe, R.D., Stebner, A.P. "Crack Propagation Mechanisms of an Aged Nickel-Titanium-Hafnium Shape Memory Alloy," 2019, *Scripta Materialia*, 159:85–88, 10.1016/j.scriptamat.2018.09.019.
- Amin-Ahmadi, B**.,** Pauza, J., Shamimi, A., Duerig, T.W., Noebe, R.D., Stebner, A.P. "Coherency Strains of H-Phase Precipitates and Their Influence on Functional Properties of Nickel-Titanium-Hafnium Shape Memory Alloys," 2018 *Scripta Materialia*, 147: 83–87, 10.1016/j.scriptamat.2018.01.00.
- Amin-Ahmadi, B**.,** Gallmeyer, T**.,** Pauza, J., Duerig, T., Noebe, R.D., Stebner, A.P. "Effect of a Pre-Aging Treatment on the Mechanical Behaviors of Ni50.3Ti49.7 − xHfx (x ≤ 9 at.%) Shape Memory Alloys," 2018, *Scripta Materialia*, 147:11–15, 10.1016/j.scriptamat.2017.12.024
- Casalena, L., Bucsek, A.N., Pagan, D.C., Hommer, G.M., Bigelow, G.S., Obstalecki, M., Noebe, R.D., Mills, M.J., Stebner, A.P. "Structure-Property Relationships of a High Strength Superelastic NiTi–1Hf Alloy," 2018, *Advanced Engineering Materials*, 20(9):1800046, 10.1002/adem.201800046.
-

List of the travel to the beam lines and use of the DOE User facilities:

1. February 2017: 3D X-ray diffraction at BL F-2, Cornell High Energy Synchrotron Source.
2. August 2017: 3D X-ray diffraction at BL 1-ID-E, Advanced Photon Source, Argonne National Laboratory.
3. Dec 2017: X-ray microLaue diffraction at BL 12. 3.2, Advanced Light Source, Lawrence Berkeley National Laboratory.

List of students/postdocs trained:
Harshad: Research Engineer, Confluent Medical Technologies.
Partha: Postdoctoral Scholar at Stanford Synchrotron Radiation Lightsource, SLAC National Accelerator Laboratory.

> *PhD Thesis: Influence of Multiscale Constraint on Inelastic Deformation Behavior of Austenite and Martensite Phases in Shape Memory Alloys. Defended on 08/01/2018.*

contact info: Cate Brinson, Duke University, cate.brinson@duke.edu

upload file: (the rest of this document)

The following research findings were published / are in review as a result of Phase II funding:

1. Paul, P.P. Paranjape, H.M. Nobumichi, T. Chumlyakov, Y.I. Brinson, L.C. "In-situ, microscale characterization of heterogeneous deformation around notch in martensitic Shape Memory Alloy" 2019, Materials Science and Engineering: A (in press).

   Materials Science Highlights:

   - Deformation characterization of low-symmetry phases such as martensite in SMAs is challenging due to a finescale hierarchical microstructure.
   - Using X-ray microLaue diffraction, in-situ deformation of martensite is examined in a notched NiTi specimen.
   - The local deformation is influenced by the notch stress field, initial martensite microstructure, and interaction between notch stress field and the external load.
   - The microstructure evolves heterogeneously and inelastically, with detwinning and twin nucleation occurring simultaneously through loading.
   - These results contrast with the traditional view of martensite deformation that is partitioned in three distinct regimes: elasticity, reorientation and de-twinning.

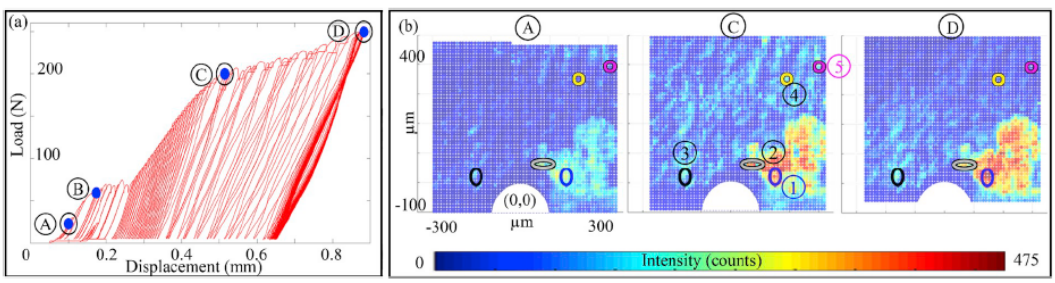

Fig. 2. (a) The nominal load-displacement curve. Loading was interrupted at 15 N,55 N, 200 N and 250 N to obtain diffraction scans. (b) The spatial distribution of the average diffraction intensity (signal to noise ratio) at three of the four load steps. These plots span the area indicated by the dotted box in Fig. 1(b). The five numbered areas, marked by colored ellipses are analyzed in further detail in Fig. 3. (For interpretation of the references to colour in this figure legend, the reader is referred to the web version of this article.)

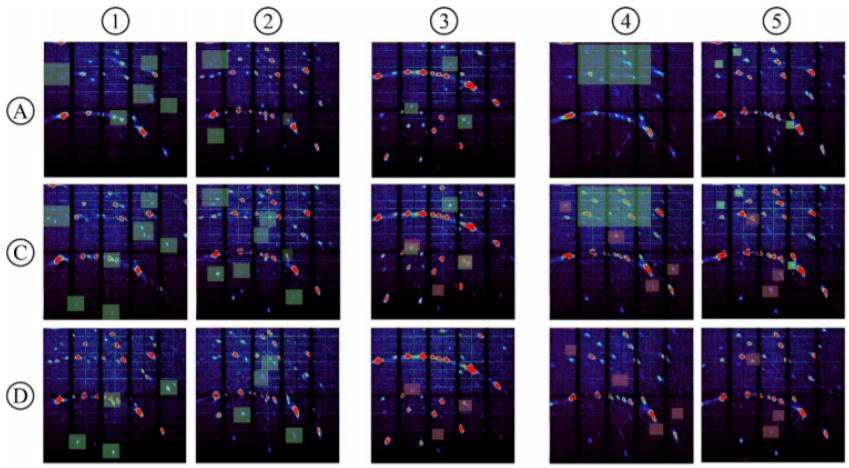

Fig. 3. Evolution of diffraction patterns with loading at the five numbered locations at loading steps Ⓐ, Ⓒ and Ⓓ, as shown in Fig. 2(b). Columns ① and ② lie to the top right of the notch, in the region of high average deformation intensity. The central column (③) lies to the top left of the notch. Columns ④ and ⑤ indicate regions relatively far away from the notch, to the top right of the diffraction area. Green boxes indicate appearance of new spots while purple boxes highlight the disappearance of existing spots. (For interpretation of the references to color in this figure legend, the reader is referred to the Web version of this article.)

2. Paranjape, H.M., Paul, P.P., Amin-Ahmadi, B., Sharma, H., Dale, D., Ko, J.Y.P., Chumlyakov, Y.I., Brinson, L.C., Stebner, A.P. "In Situ 3D Characterization of the Deformation Mechanics of a Superelastic NiTi Shape Memory Alloy Single Crystal under Multiscale Constraint," 2018, Acta Materialia, 144:748–757, 10.1016/j.actamat.2017.11.026.

Materials Science Highlight:

- Load shedding about carbide inclusions, coherent nanoprecipitates, and subgrain boundaries was characterized with 3D-xray diffraction and modeling techniques and shown to "frustrate" phase transformations in the case of inclusions – leading to non-optimal martensite microstructures. Precipitates and subgrains, however, do not significantly impede the phase transformations.

Technique Highlights:

- 3D X-ray diffraction techniques were used to directly study low symmetry (monoclinic) crystals within a polycrystal. The diffraction analysis techniques needed for such studies are documented in this paper for the broader scientific community.
- A technique for statistically comparing effects of inclusions using simulations of a simplified crystal-scale finite element model to interpret more complex signals in 3D X-ray diffraction data were developed and documented.

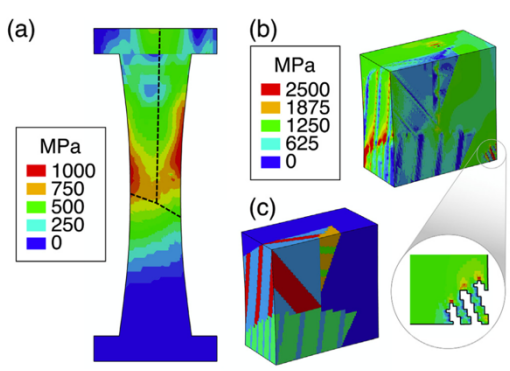

Fig. 5. Microstructural simulation results. (a) Axial stress at 600 MPa macro stress. B2 low-angle grain boundaries are shown by dashed lines. (b) A section of the gage showing details of local stress at 800 MPa macro stress. The inset shows the heterogeneous axial stress around an inclusion array. The inclusion itself is not shown. (c) The B19′ microstructure corresponding to the section in (b). Blue regions correspond to B2. Other colors correspond to various B19′ CVs. (For interpretation of the references to colour in this figure legend, the reader is referred to the web version of this article.)

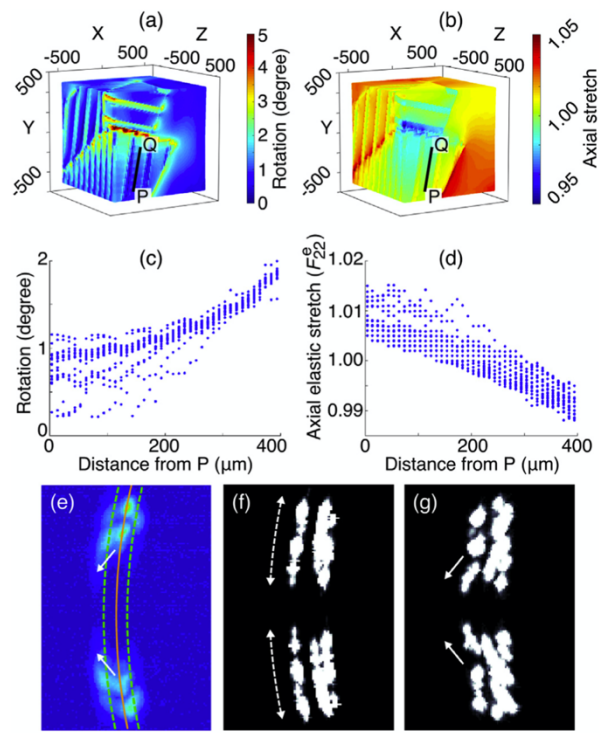

Fig. 9. Local elastic stretch and rotation in the B19′ phase vary systematically in the twin bands as a function of the distance from the nearest phase interface. (a) Rotation at 800 MPa macro axial stress in the simulations. (b) Axial elastic stretch at the same macro stress. (c) Rotation along a path PQ in one martensite CV. (d) Axial elastic stretch along the same path PQ. (e) Experimental spot patterns at peak stress. Austenite spots are along the solid orange arc. Martensite spots are along the dashed green arcs. Martensite spots show systematic elongation in both radial and azimuthal directions. (f) Simulated spot patterns using only the rotation information from the microstructural simulation at 800 MPa macro axial stress show azimuthal elongation (dashed arrow), but not radial elongation. (g) Simulated spots show both radial and azimuthal spread similar to (e) when both rotation and elastic stretch from the microstructural simulations are considered. (For interpretation of the references to colour in this figure legend, the reader is referred to the web version of this article.)

3. Paul, P.P., Fortman, M., Paranjape, H.M., Anderson, P.M., Stebner, A.P., Brinson, C.L. "Influence of Structure and Microstructure on Deformation Localization and Crack Growth in NiTi Shape Memory Alloys," 2018, *Shape Memory and Superelasticity*, 4(2):285–293, 10.1007/s40830-018-0172-1.

This paper was awarded the "2018 Editor's Choice Article Award."

Materials Science Highlights:

- The initiation and growth of martensite bands about stress concentrations (holes) was found to be strongly influenced by polycrystalline texture. Specifically, with crystals orientated favorable for transformation about a defect, the martensite bands nucleated as expected due to the stress concentration caused by the hold; however, crystals oriented unfavorable for transformation cause the bands to nucleate and grow in torturous paths despite the macroscopic stress favoring transformation.
- Cracks strongly prefer to grow through grains with [110] crystal lattice directions aligned with the loading direction.

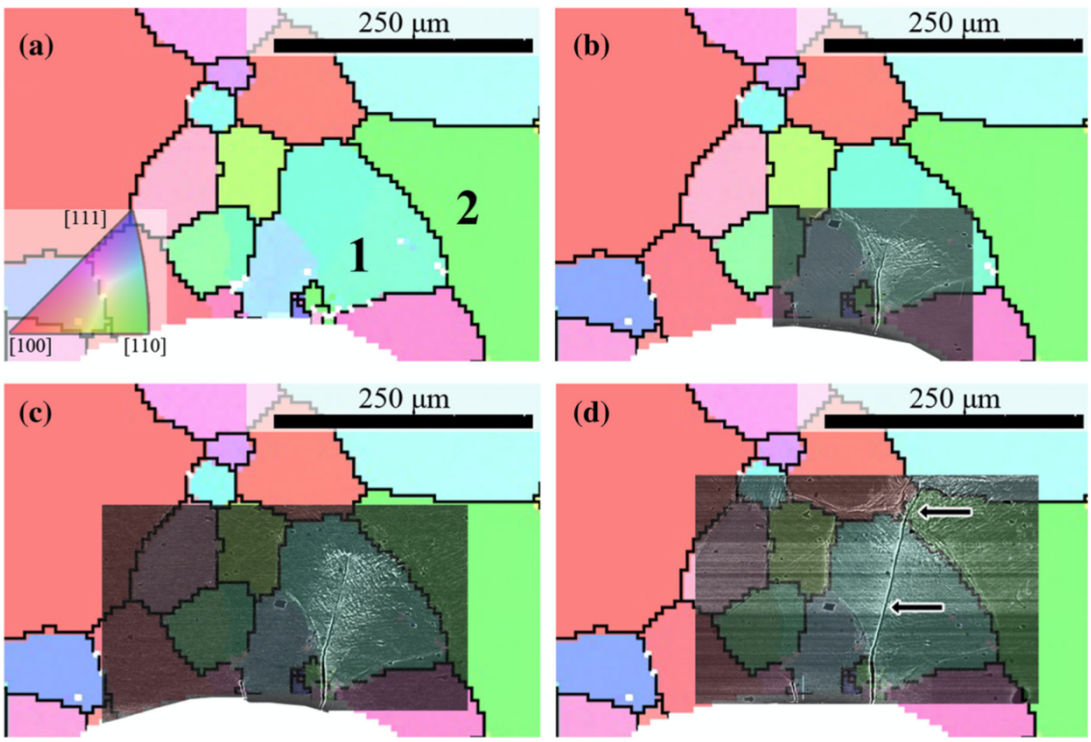

Fig. 5 Crack growth in the top left quadrant shown by the dotted box in Fig. 1a. **a** Grain orientation with respect to the leading axis. The standard coloring scheme is used, as shown in the key in Fig. 1b. Crack geometry, as seen using ex situ SEM after **b** 20 cycles, **c** 50 cycles, and **d** 100 cycles. The crack in the aquamarine grain (numbered 1) grows through a straight path through the entire grain until it reaches a grain boundary, and then it continues to grow into the green grain (numbered 2). The arrows in (**d**) indicate the change in angle of the crack as it grows from Grain 1 to Grain 2. Residual deformation is seen around the crack (Color figure online)

4. Paul, P.P. Paranjape, H.M., Amin-Ahmadi, B., Pagan D.C., Chumlyakov, Y.I. Brinson, L.C. "Heterogeneity and Inelasticity of Multiscale Deformation in a Notched Martensitic NiTi Shape Memory Alloy Specimen" 2019, Acta Materialia (In review).

   Materials Science Highlights:

   - We investigate the deformation in a notched martensitic (monoclinic) NiTi shape memory alloy specimen using in-situ and ex-situ nano- to macro-scale characterization techniques and a macro-scale simulation.
   - At the macroscale, we demonstrate that the deformation of martensite in the notched specimen is largely determined by the structural features, and the hierarchical nature of the microstructure plays a smaller role.
   - At the micro-scale, the martensite microstructure continuously evolves during tensile loading. However, the nano-scale twin laminate structure persists despite the large imposed deformation and the presence of stress concentrating features such as a notch.
   - At the nanoscale, we show localized amorphization/nanocrystallization as the primary mechanism of martensite deformation in the immediate vicinity of the notch. Slightly further away, there is a persistence of the twin structure even up to fracture.
   - The persistence of a nano-laminate structure at high loads, rather than coarsening into large domains of individual martensite variants indicates that the deformation field around cracks or notches in martensite may be modeled with adequate accuracy using coarse-grained models.

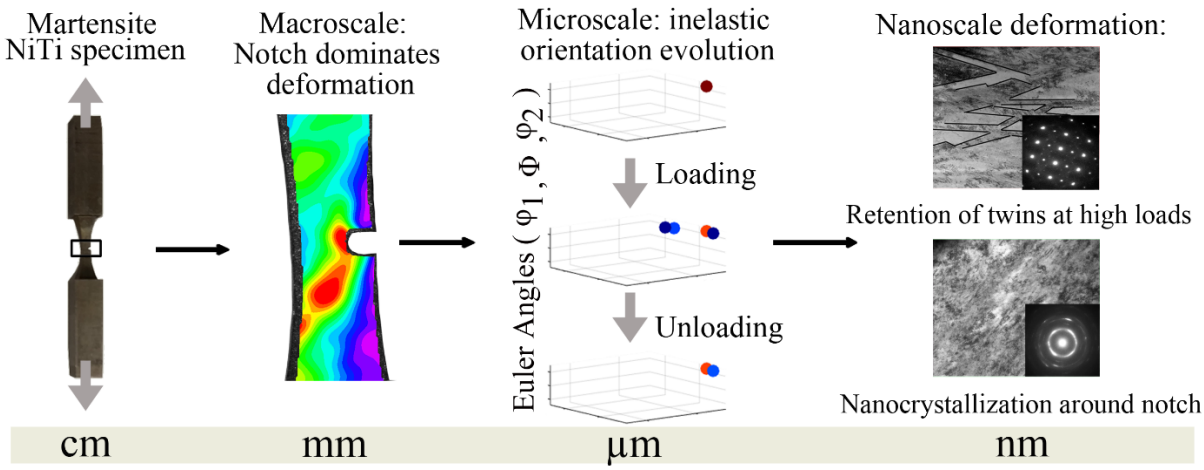

Fig: Multiscale characterizations on inelastic deformation leading up to fracture in low-symmetry martensite phase in NiTi, during tensile loading. The techniques spanning across length scales involve macroscale strain measurement (Digital image Correlation), microscale orientation (high energy X-ray diffraction) and nanoscale twin structure (TEM), showing a heterogeneous and continuously evolving microstructure.

The support of the grant also enabled L. C. Brinson to collaborate on this related research (as acknowledged in the publications):

5. Paul, P.P., Kabirifar, P, Sun, Q.P., Brinson, L.C. “Structure-microstructure interactions in compression deformation of NiTi shape memory alloy micropillars,” 2019, Materials Letters, 257:126693, https://doi.org/10.1016/j.matlet.2019.126693.

   Materials Science Highlights:
   - Micromechanical simulations elucidate structure-microstructure interactions in SMAs.
   - Deformation is suppressed when grain size(G) ~ specimen size(D) in SMA micropillars.
   - Structure: Specimen geometry interaction with grain size is strongest when G~D.
   - Microstructure: Texture and neighboring grains’ interaction is weaker when G~D.
   - Strong structural and weak microstructural effects cause lower overall deformation.

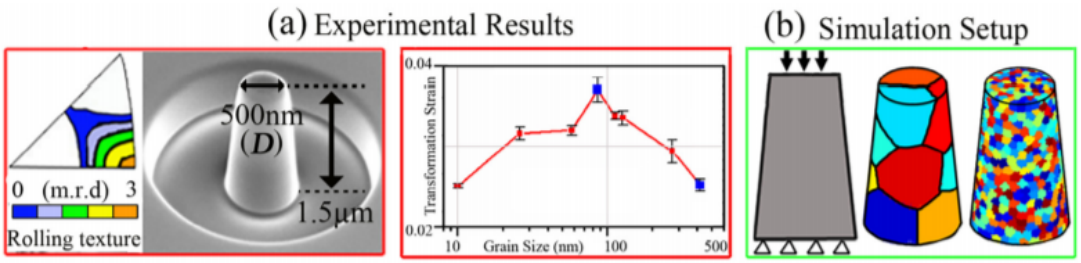

Fig. 1. (a) Experimental micropillar with cold-rolled texture [8], showing the dependence of deformation on ***GS*** [5] at a nominal stress of 1500 MPa. (b) The grayscale specimen shows a 2D slice of the simulation with boundary conditions while the colored figures show grains (colored randomly) with ***GS*** 421 nm and 86 nm.

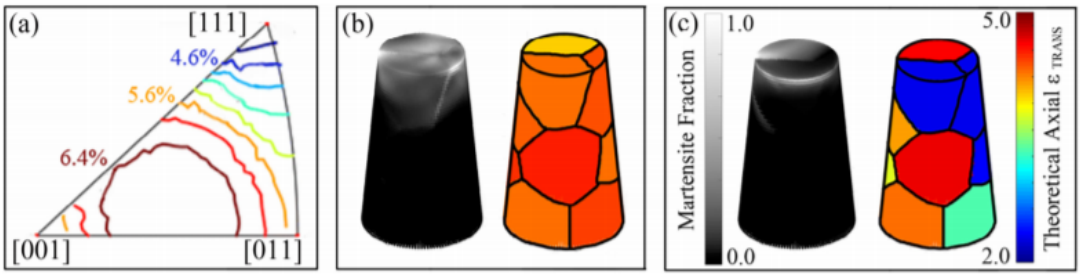

Fig 2. (a) Theoretical ε_{trans} produced by grains, colored by orientation w.r.t the loading axis [12]. (b) Experimental specimen with cold-rolled texture. (c) Theoretical specimens with random polycrystal texture, showing lesser deformation (white regions) compared to (b). In b-c, the grayscale and colored contours show ***MF*** and theoretical ε_{trans} respectively, with ***GS*** 421 nm.

Finally, the support of the grant also enabled A.P. Stebner to collaborate on this related research (as acknowledged in the publications):

6. Amin-Ahmadi, B., Noebe, R.D., Stebner, A.P. "Crack Propagation Mechanisms of an Aged Nickel-Titanium-Hafnium Shape Memory Alloy," 2019, *Scripta Materialia*, 159:85–88, 10.1016/j.scriptamat.2018.09.019.

Materials Science Highlights:

- A crack growing through stress-induced martensite prefers to grow along <011> type II twin planes, but coherent H-Phase nanoprecipitates act as obstacles, causing cracks to jog around them, between twin planes. Hence, a microstructure with a more dense precipitate network is expected to exhibit higher toughness.
- About the crack tip, NiTiHf is amorphous. Slightly further away, nanocrystals are stabilized in the amorphous phase. Then longer range, the expected austenite/martensite structures and interfaces are present. Ni-enrichment is found in the amorphous region.

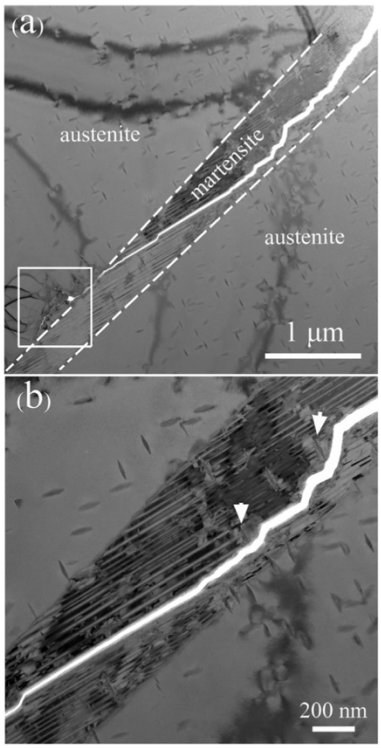

Fig. 2. (a) conventional BF micrograph showing a crack within the martensite phase of the NiTiHf alloy and (b) high magnification BF image showing the crack path along ⟨011⟩ type II twin planes. The crack is interrupted when it encounters H-phase precipitates (indicated by white arrows) and redirected to another twin boundary creating a torturous crack path.

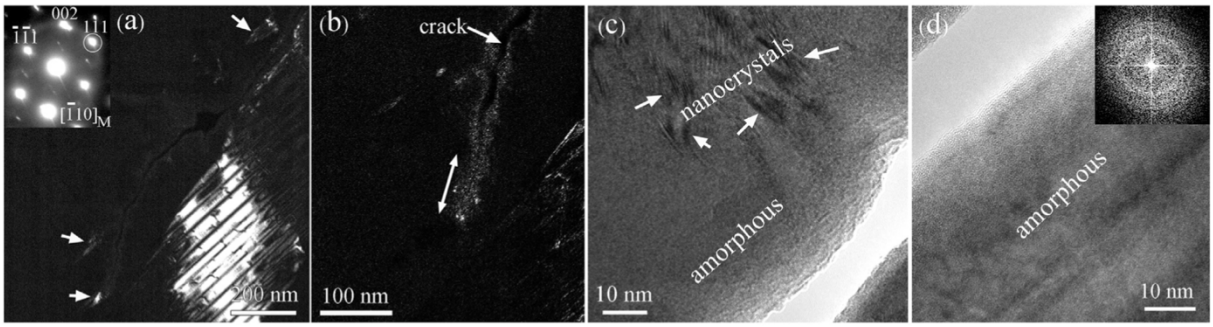

Fig. 3. (a) central DF micrograph imaged using $g = (111)_{B19'}$ showing the nano-sized stress-induced martensite formed inside the austenite phase near the crack edge. (b) magnified DF image around the crack tip highlighting structure in the amorphous diffraction condition. (c) HRTEM micrograph around the crack edge within the austenite phase, showing amorphous region immediately next to the crack, and formation of nanocrystals (indicated by white arrows) within the edge of the amorphous region. (d) HRTEM micrograph around the crack edge within the martensite phase showing the amorphous region, but the absence of nanocrystals.

7. Amin-Ahmadi, B., Pauza, J., Shamimi, A., Duerig, T.W., Noebe, R.D., Stebner, A.P. "Coherency Strains of H-Phase Precipitates and Their Influence on Functional Properties of Nickel-Titanium-Hafnium Shape Memory Alloys," 2018 *Scripta Materialia*, 147: 83–87, 10.1016/j.scriptamat.2018.01.00.

Materials Science Highlights:

- Growth of H-phase nanoprecipitates from 1nm to 10 nm is found to increase transformation temperatures primarily through a Clausius-Clapeyron driven mechanism of increasing coherency strain field magnitudes. Then, as the precipitates are further coarsened, their interfaces become less coherent and misfit dislocations form on the interfaces, relaxing the coherency strains, which is accompanied by a drop in transformation temperatures.

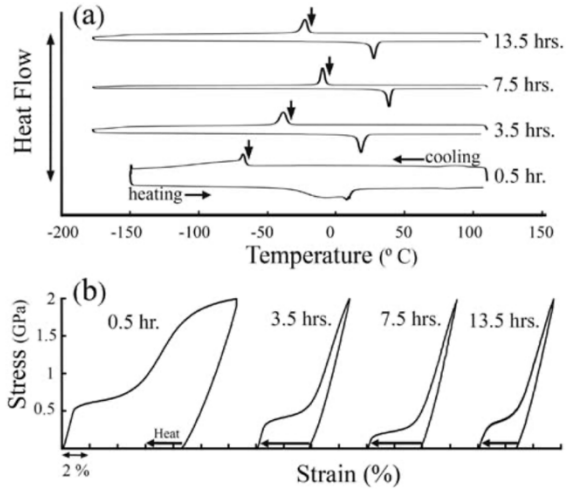

Fig. 1. Effect of aging time at 550 °C on (a) the transformation temperatures and (b) superelastic behavior of $Ni_{50.3}Ti_{41.7}Hf_8$ alloy. M_s is indicated by arrows in each DSC curve.

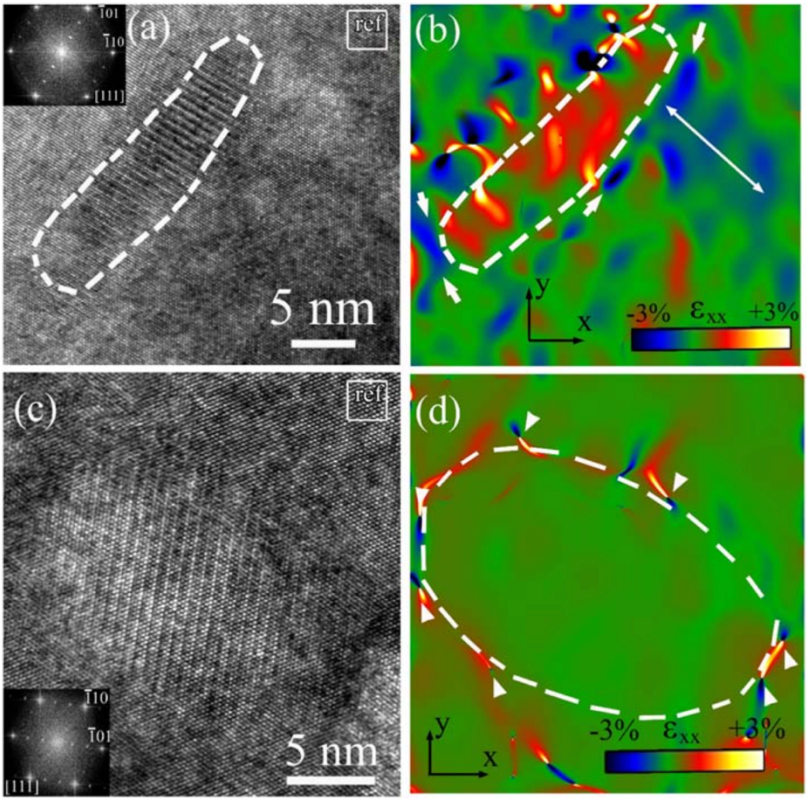

Fig. 3. HRTEM micrograph taken along $[111]_{B2}$ zone axis showing H-phase precipitate and corresponding GPA map of ε_{xx} component in $Ni_{50.3}Ti_{41.7}Hf_8$ alloy after aging at 550 °C for (a,b) 3.5 h and (c,d) 13.5 h. The unstrained region as a reference structure for GPA analysis is also indicated by the white squares in (a) and (c).

8. Amin-Ahmadi, B., Gallmeyer, T., Pauza, J., Duerig, T., Noebe, R.D., Stebner, A.P. "Effect of a Pre-Aging Treatment on the Mechanical Behaviors of Ni50.3Ti49.7 − xHfx (x ≤ 9 at.%) Shape Memory Alloys," 2018, *Scripta Materialia*, 147:11–15, 10.1016/j.scriptamat.2017.12.024

Materials Science Highlights:

- A diffusional "pre-aging" heat treatment, at a temperature just below the precipitation temperature of H-phase nanoprecipitates, is found to promote more homogenous nucleation and growth of the nanoprecipitates upon subsequent aging. Specifically, Hf clusters within the matrix as a result of pre-aging, and those clusters then serve as nanoprecipitate nuclei upon aging.

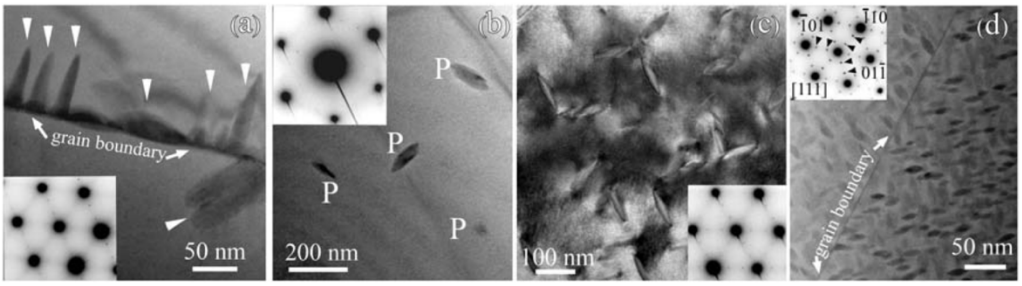

Fig. 3. Conventional BF images of (a, b) $Ni_{50.3}Ti_{42.7}Hf_6$, (c) $Ni_{50.3}Ti_{41.2}Hf_{8.5}$, and (d) $Ni_{50.3}Ti_{40.7}Hf_9$ after aging at 550 °C for 3.5 h without the pre-aging treatment. All corresponding SAED patterns shown in each insets are along the [111] zone axis of the B2 structure. The fundamental reflections are indexed at the inset of Fig. 3d and the super reflections originated from H-phase precipitates are marked with arrowheads.

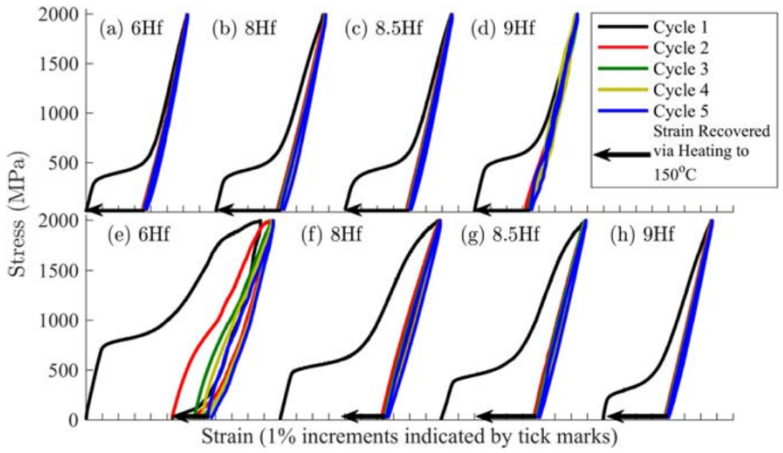

Fig. 1. Mechanical behavior of $Ni_{50.3}Ti_{42.7}Hf_6$, $Ni_{50.3}Ti_{41.7}Hf_8$, $Ni_{50.3}Ti_{41.2}Hf_{8.5}$, and $Ni_{50.3}Ti_{40.7}Hf_9$ (at. %) alloys in compression with (a–d) and without (e–h) the pre-aging treatment at 300 °C for 12 h followed by normal aging at 550 °C for 3.5 h for all samples.

9. Casalena, L., Bucsek, A.N., Pagan, D.C., Hommer, G.M., Bigelow, G.S., Obstalecki, M., Noebe, R.D., Mills, M.J., Stebner, A.P. "Structure-Property Relationships of a High Strength Superelastic NiTi–1Hf Alloy," 2018, *Advanced Engineering Materials*, 20(9):1800046, 10.1002/adem.201800046.

Materials Science Highlights:

- A new NiTiHf alloy is found to exhibit near-zero hysteresis and higher strength than comparable binary NiTi alloys despite having austenite/martensite crystal structures that are not compatible with each other. Interfacial dislocations stabilize the formation of interfaces between single austenite and martensite domains, and enable these remarkable superelastic properties.

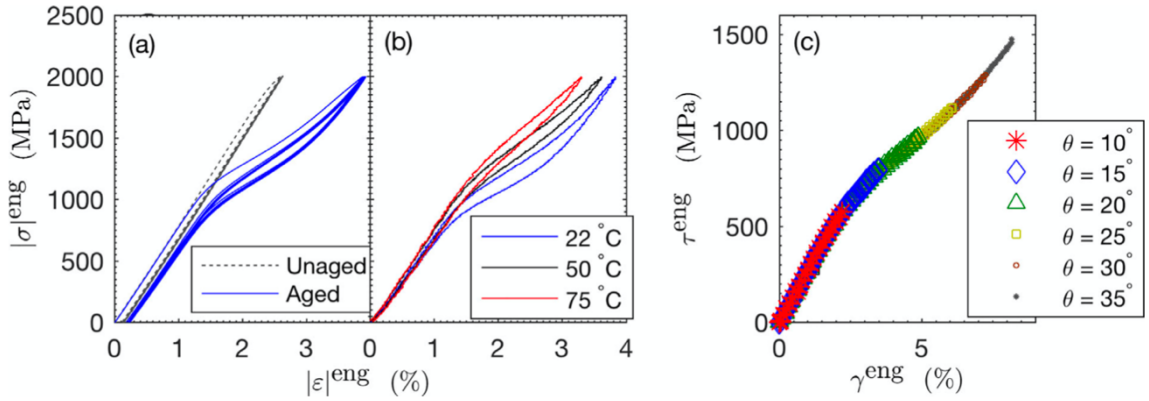

Figure 1. $Ni_{54}Ti_{45}Hf_1$ mechanical responses are shown. a) Compression responses of an unaged sample cycled 10 cycles and an aged sample cycled 5 cycles at the same strain rate at room temperature showed little accumulation of plastic strain after the first cycle in either case. The unaged sample exhibited linear-elastic behavior after cycle 1 while the aged sample showed macroscopic superelasticity. b) The stress for initiating superelasticity increased with increasing temperature. c) The room temperature mechanical response of an aged sample torqued at a constant rotation rate to increasing angles demonstrates an analogous superelastic response in shear.

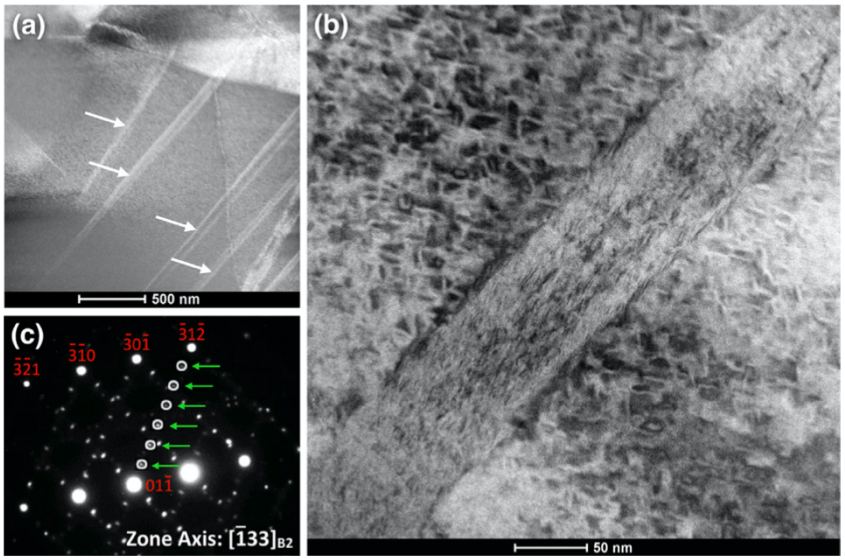

Figure 4. a) Dark-field STEM image of the aged, 10-cycle-tested $Ni_{54}Ti_{45}Hf_1$ alloy showing martensite streaks crossing low-angle grain boundaries. b) Higher magnification micrograph showing a martensite lath within the matrix containing a very high density of Ti_3Ni_4 precipitates on the size scale of 10–30 nm. c) TEM selected area diffraction pattern of a matrix region exhibiting the characteristic $n/7\{321\}$ type reflections, indicated by the arrows, confirming the rhombohedral structural characteristic of the Ti_3Ni_4 precipitates.